Developing a keV Electron Diode Source

L. Concini [1], J. Matthew Gjevre[1], C. Guthrie[1], Dr. R. Fedosejevs[1]

[1]Department of Electrical and Computer Engineering, University of Alberta, Edmonton, Canada

Introduction

Motivation

The RADICALS satellite mission, led by Dr. Ian Mann in conjunction with several Canadian universities, will study the impact of space radiation on Earth's climate. To calibrate its detectors, a reliable keV-range electron source, or an "electron gun", is required to fire electrons with energies in the thousands of electron volts.

Objectives

This project involves the design and development of a keV electron source to generate high energy electrons. We will:

1. Optimize diode geometry for straight electron paths;
2. Implement high-voltage circuitry and housing;
3. Navigate electric breakdown in the high-voltage setup;
4. Test the final design and identify future improvements.

Design

Electron Trajectory Simulation

We evaluated how different capacitor geometries affect electron trajectories as they travel from the cathode to escape through the anode. Electrostatics were solved using Finite Element Method Magnetics (FEMM), and electron trajectories were tracked using a Runge-Kutta 4 integrator simultaneously solving a system of relativistic differential equations [1].

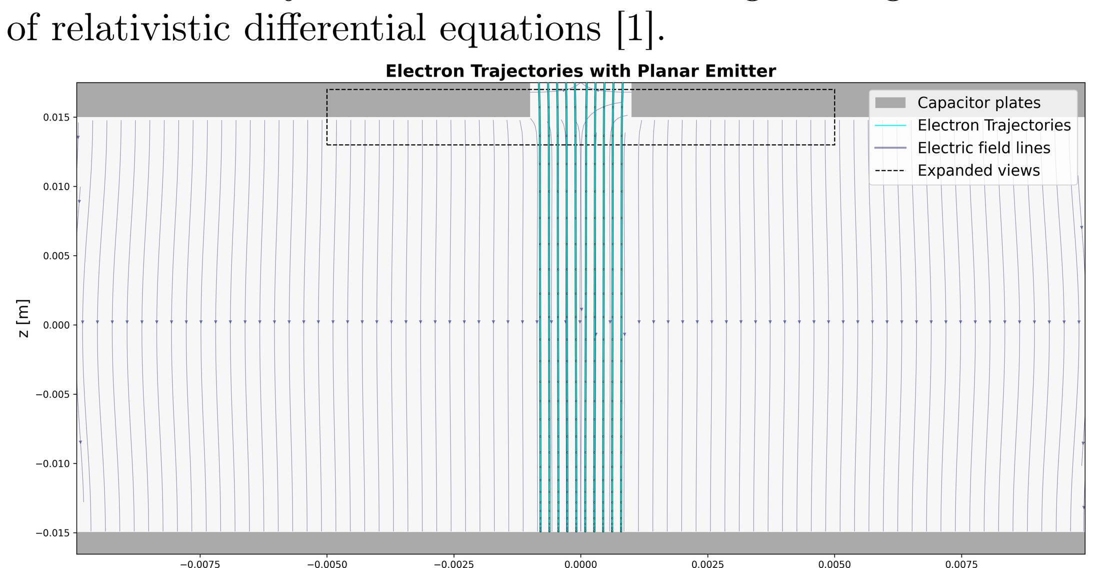

Figure 1: Flat cathode geometry producing a collimated electron beam.

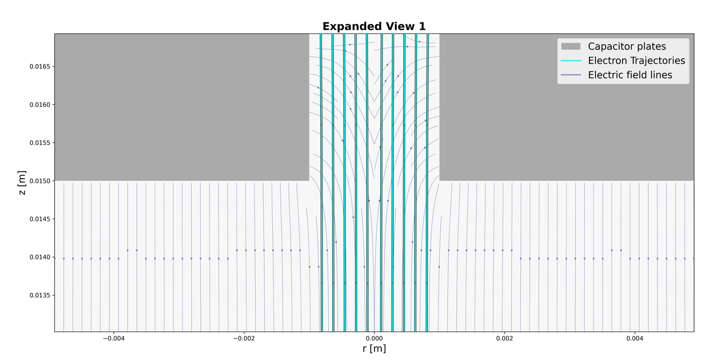

Figure 2: Expanded view of collimated exit beam.

Notably, the flat cathode in Figure 1 produced the straightest electron paths with almost no beam divergence. An anode with a small circular hole consistently allowed this collimated beam to escape.

Generating High Voltage

Achieving N keV electron energies requires an N kV DC voltage across our diode. A driver circuit converts a 6 V battery input into a $\sim$6 kV peak-to-peak sine wave. We built a 7-stage Cockcroft-Walton voltage multiplier to step this AC signal up to a $\sim$45 kV DC output. Each stage adds $2V_p$ to the DC output, where V_p is the peak amplitude of the AC source. The ideal voltage of output node D_4 relative to ground is:

$$V_{\text{out}} = 2nV_p \quad (1)$$

Where n is the number of stages. In testing, we found the driver could sustain seven stages before corona leakage stopped further multiplication.

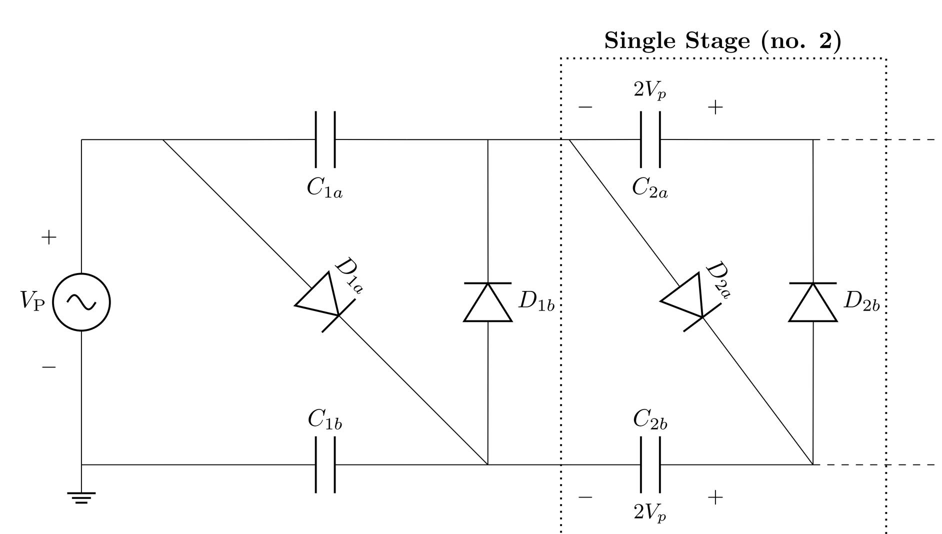

Figure 3: Cockcroft-Walton voltage multiplier circuit diagram, highlighting one modular stage.

Mitigating Breakdown

We theoretically and experimentally addressed electrical arcing by considering three factors.

Paschen's Law

Paschen's Law specifies the breakdown voltage of a gas, via ionization of the gas particles in a large potential difference [2].

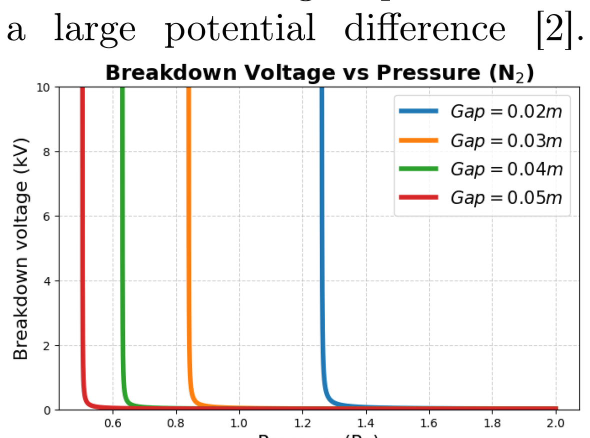

Figure 4: A Paschen curve using parameters estimated from literature [3].

Below $1Pa$, the breakdown voltage increases very quickly. However, this model ignores cathode surface condition and outgassing, which may cause localized environmental fluctuations. The true vacuum limitations of our system must be explored experimentally.

Field Emission

Field emission analyses breakdown due to quantum tunnelling of electrons under a high potential difference.

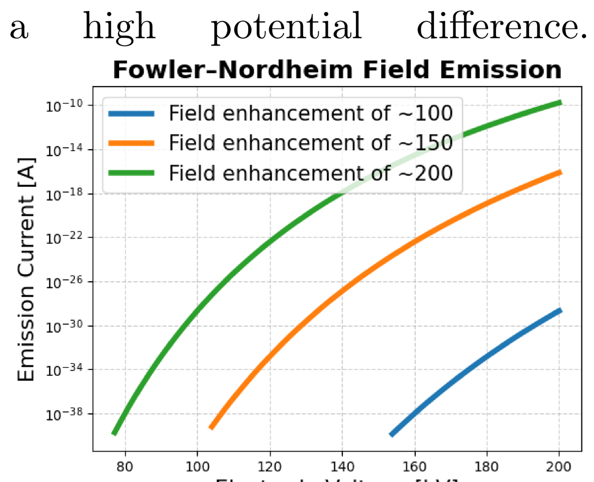

Figure 5: Fowler-Nordheim field emission curves.

Field emission levels rely on the local field enhancement factor β due to microscopic material defects [4]. Estimated parameters from literature imply low field emission, however the non-linear response is susceptible to small changes.

Outgassing

Outgassing is the release of trapped vapours from components in a vacuum chamber, which may increase local pressure.

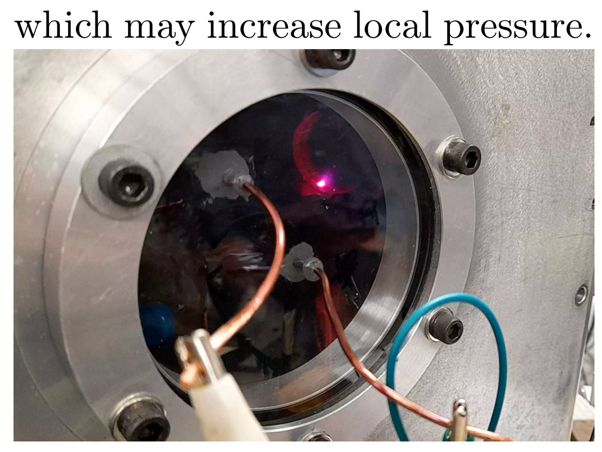

Figure 6: Reddish-pink glow discharge due to outgassing.

Preliminary test showed breakdown around plastic components, with a net chamber pressure of $0.1Pa$, below our Paschen breakdown estimate. Replacing high-outgassing plastics and improving vacuum down to $0.002Pa$ stopped breakdown.

Methods

We completed a full vacuum test of our revised prototype, measuring the high-energy particle production with a MiniPIX radiation detector.

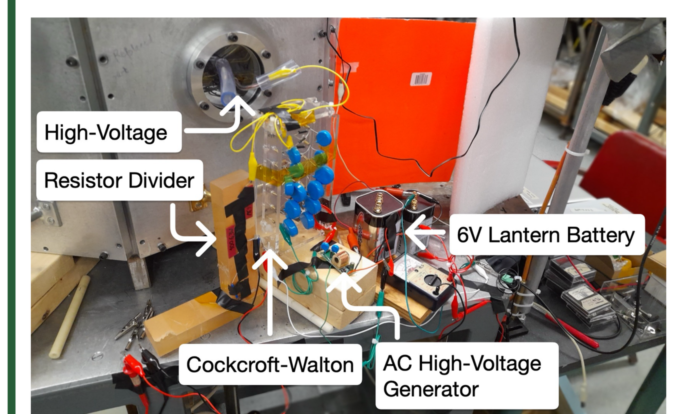

Figure 7: The final arrangement of our circuit elements outside the vacuum chamber.

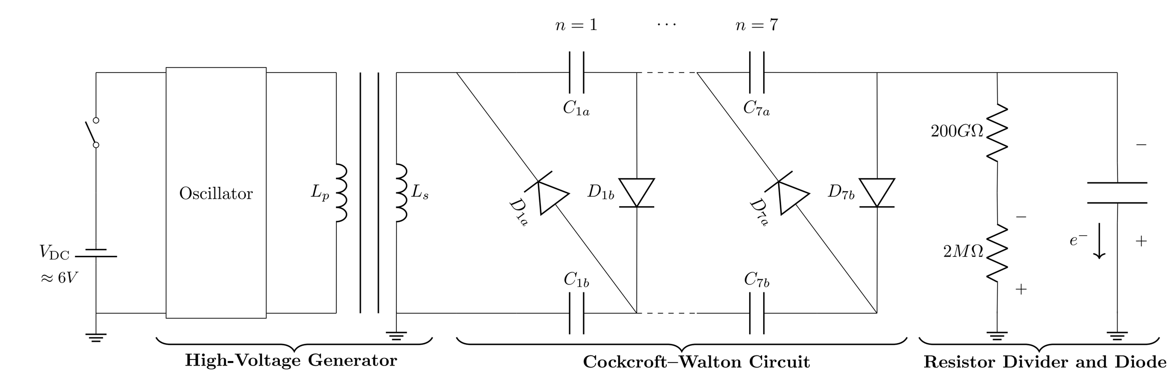

Figure 8: Circuit diagram of our final testing setup. The diodes are inverted compared to a canonical Cockcroft-Walton circuit, as we hold the cathode at a *negative* potential with respect to the grounded anode.

Outside the chamber, we connected our circuit as shown in Figure 8. We used a $200G\Omega : 2M\Omega$ resistor divider to measure diode voltage.

We assembled the diode inside the vacuum chamber and aligned it with the MiniPIX with a $6\mu m$ aluminium foil filter to block $< 22kV$ electrons. To mitigate Paschen breakdown and field emission, the cathode was sanded with 200 grit sandpaper, and the vacuum was drawn to $0.0020Pa$. We aligned a UV laser and mounted UV light with the center of the cathode.

We completed 10 second measurements for various diode voltages, using the MiniPIX to capture particle detection locations and energies. We varied the status of the room lights, UV light, and the UV laser.

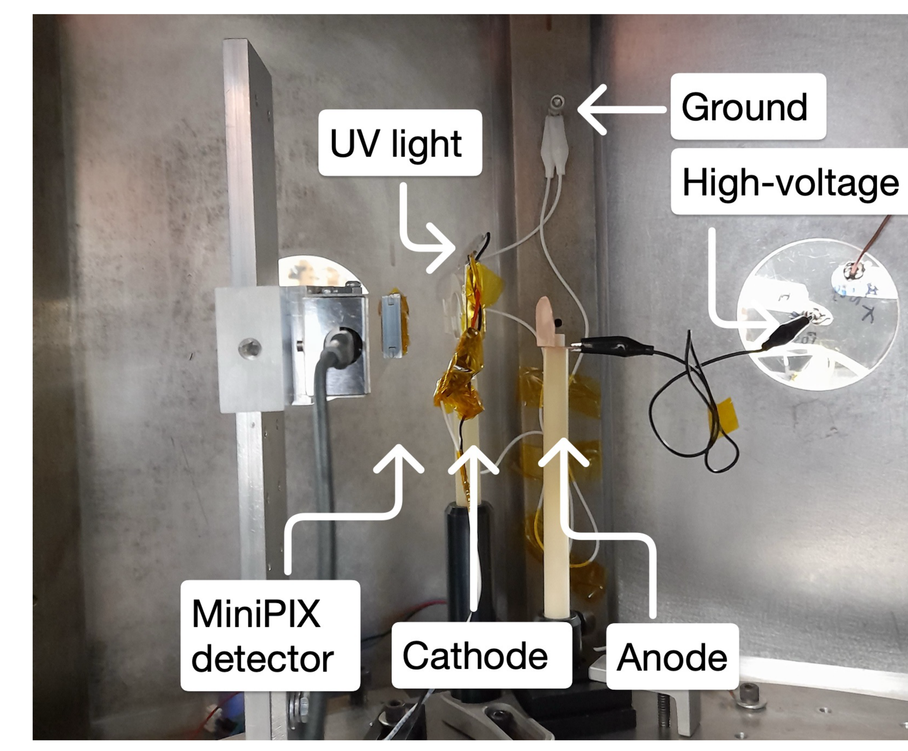

Figure 9: A side view of the final arrangement of our diode setup.

Results

A heat map of particle detection locations on the MiniPIX sensor reveals sparse background radiation detections, with pixels activated for at most 4% of trials. Activating the diode produces a cluster of impacts near the centre with pixels active for 80% of trials. Detection frequency contour rings illustrate concentric circular arcs produced by the circular opening of the anode. Farther detections are diffuse as they are increasingly composed of scattered electrons and bremsstrahlung produced by electron-anode collisions.

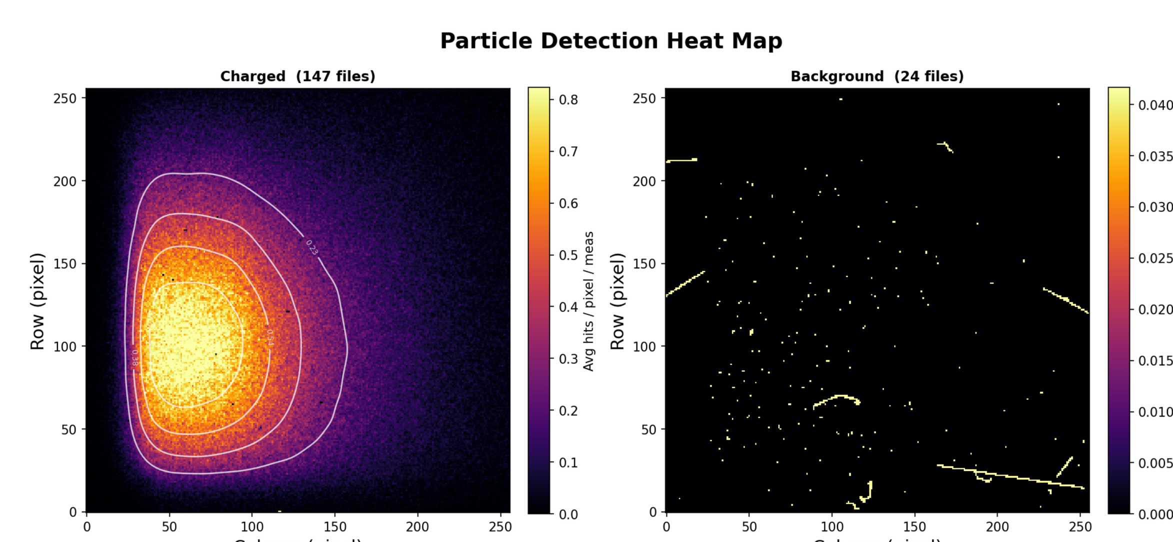

Figure 10: Heatmap of particle detections by the MiniPIX radiation detector reveals a semi-collimated beam. The sensor's mounting frame shields a ~ 20 pixel border around the device, leaving a shaded square band.

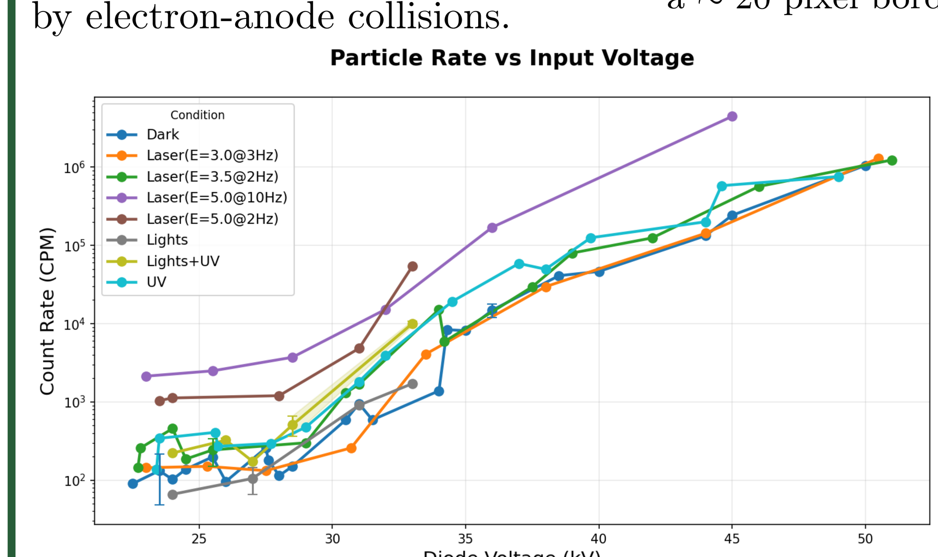

Figure 11: Log plot of particle detection rate against diode voltage reveals strong cathode self-emission.

Figure 11 confirms a sharp-drop off in detections below $\sim 30kV$, due to the $6\mu m$ aluminium foil filter on the MiniPIX. The $5W$ UV laser and UV light result in an order of magnitude and a factor of two increase in particle count rates over our self-emission tests, respectively. However, all emissions exponentially increase with voltage. This indicates a high rate of self-emission from the cathode, even without photo excitation. The sensor's mounting frame shields a ~ 20 pixel border around the device, leaving a shaded square band.

Field emission has a highly non-linear relationship with β, the local field enhancement parameter that relies on micro-scale surface smoothness and material defects. Our count rate corresponds with a $\beta \approx 800$ from Figure 5, which exceeds our initial estimates [5]. Figure 12 shows that increasing diode voltage linearly increases median particle energy. The slope of $m = (0.58 \pm 0.03)\,\frac{keV}{kV}$ is less than the ideal slope of $1\frac{keV}{kV}$. This indicates consistent electron scattering and bremsstrahlung production, which broadens the energy spectrum and skews the median downwards from the theoretical slope of $1\frac{keV}{kV}$.

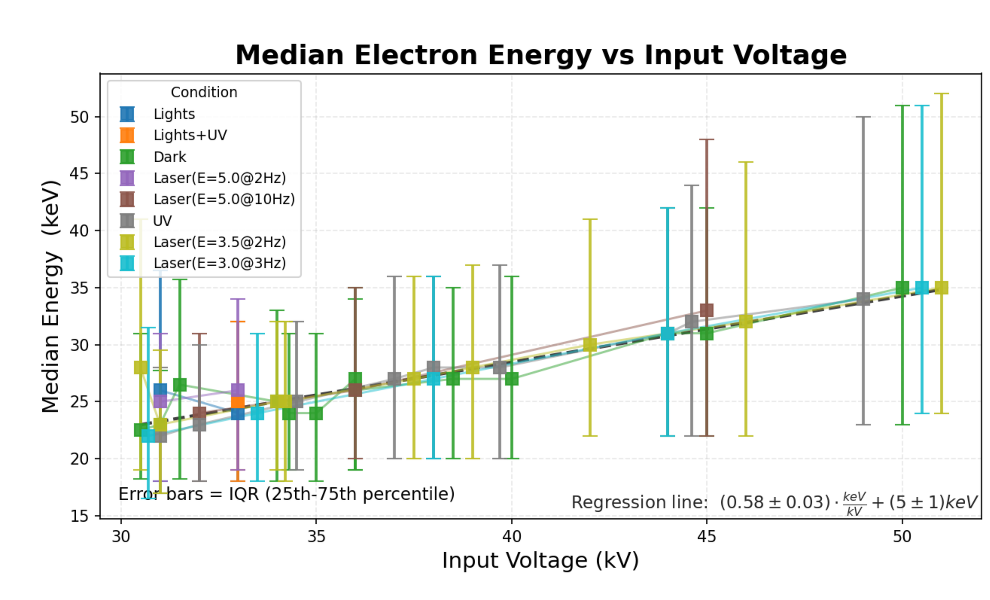

Figure 12: Scatter plot relating the median energy of detected electrons to voltage across the diode. Linear fit $y = (0.58 \pm 0.03)\,\frac{keV}{kV} \cdot x + (5 \pm 1)\,keV$.

Conclusions

We identified several improvements to advance our prototype towards accurate calibration of high-energy space particle detectors:

→ While the diode successfully produces a semi-collimated radiation beam incident on the particle detector, a thick lead aperture behind the anode could absorb x-rays from scattered electrons, removing the diffuse noise cloud on the detector.

→ A magnetic spectrometer could filter only the highest-energy particles from the diode source.

→ Polishing the cathode surface would reduce β, decrease field emission flux, facilitate accurate particle selection, and raise the breakdown pressure threshold.

→ A higher-voltage oscillator driving the Cockcroft-Walton multiplier would increase the maximum attainable electron energies.

References & Acknowledgements

References

[1] J. C. Butcher, *Numerical methods for ordinary differential equations.* John Wiley & Sons, 2016.

[2] A. J. Lichtenberg, *Principles of Plasma Discharges and Materials Processing.* Wiley-Interscience, 2005.

[3] H. Bruining and J. De Boer, "Secondary electron emission of metals," *Physica*, vol. 5, no. 1, pp. 17–30, 1938.

[4] M. Radmilović-Radjenović et al., "The effect of field emission on breakdown voltage characteristics of air microdischarges,"

[5] C. M. Lampert, "Materials and molecular research division,"

[6] K. Duncan-Chamberlin, "High-voltage testing for a high-current electron gun," 2013.

Acknowledgements

I thank my supervisor, Dr. Robert Fedosejevs, for his support and high-voltage safety expertise throughout this project. I also thank graduate mentors Caleb Guthrie and John Matthew Gjevre for their invaluable guidance at each stage of the design process. I am grateful for the support of the University of Alberta Dean's Research Award Program for providing the opportunity to complete this research project.